Photonstimulated desorption and photolysis of decaborane (B10H14) at semiconductor surfaces

Housei Akazawa and Yuichi Utsumi

Citation: The Journal of Chemical Physics **104**, 8135 (1996); doi: 10.1063/1.471489
View online: http://dx.doi.org/10.1063/1.471489
View Table of Contents: http://scitation.aip.org/content/aip/journal/jcp/104/20?ver=pdfcov
Published by the AIP Publishing

Photon-stimulated desorption and photolysis of decaborane ($B_{10}H_{14}$) at semiconductor surfaces

Housei Akazawa and Yuichi Utsumi
NTT LSI Laboratories, 3-1 Morinosato Wakamiya, Atsugi-shi, Kanagawa 243-01, Japan

(Received 17 July 1995; accepted 22 February 1996)

Positive ions species resulting from photon-stimulated desorption (PSD) and photolysis from $B_{10}H_{14}$ at solid surfaces have been determined by means of time-of-flight mass spectroscopy using single-bunch operation of synchrotron radiation (SR) ($h\nu \geqslant 100$ eV). The ionic species desorbing from molecularly adsorbed $B_{10}H_{14}$ on Si(100) are H_2^+, BH_2^+, BH_3^+, and $B_2H_4^+$. During SR excited chemical vapor deposition (SR–CVD) of boron films, the primary ion products created by photolysis of $B_{10}H_{14}$ are H_2^+, $B_{10}H_x^+$, BH_x^+, and $B_9H_x^+$. From the boron films deposited by SR–CVD, the additional PSD of $B_2H_3^+$ and $B_2H_5^+$ is observed and indicates that the boron film surface is terminated by several kinds of higher-order boron hydrides. The formation of BH_3^+ and $B_2H_4^+$ is initiated by bulk-mediated secondary processes, whereas the formation of H_2^+ and $B_{10}H_x^+$ is a direct consequence of photoabsorption. The pressure dependence of the intensities of the ion species can be used to distinguish their gas and surface origins. © *1996 American Institute of Physics.* [S0021-9606(96)02220-9]

I. INTRODUCTION

Photochemistry at the surfaces of solids includes a variety of dynamical phenomena such as photoionization, photolysis, and photon-stimulated desorption (PSD). These microscopic processes are components of photoexcited chemical vapor deposition (photo-CVD), so elucidating them is valuable both as basic physics and as application-related science. Synchrotron radiation (SR)-excited Si epitaxy with Si_2H_6, studied extensively by the NTT group,[1–5] is a representative photo-CVD system making use of reactions induced by photons with energies ranging from the vacuum ultraviolet (VUV) to the soft X-ray regime. Species-specific growth kinetics in silicon CVD have been verified by employing various growth modes.[3,5] Another important application of SR–CVD is in the formation of boron films from $B_{10}H_{14}$ (Refs. 6 and 7) and from solid B_2H_6.[8] Because B atoms are light and their photoabsorption cross section in the VUV regime is therefore very low, we would expect the initial excitation in this epitaxy to be predominantly due to emitted electrons from the bulk material. Indeed, a substrate-mediated excitation mechanism was inferred from the finding of Rosenberg *et al.*[6] that the selective B film deposition is restricted to the SR-irradiated area. The B growth kinetics thus may differ remarkably from that of Si growth using disilane (Si_2H_6), in which Si deposition occurs in the nonirradiated region as well. The intermediate species pertinent to the elementary steps in the growth of B films, however, have not yet been elucidated.

Although it is generally accepted that neutral desorption predominates and ion desorption is a minor pathway, no appropriate method currently exists to detect neutrals in the field of VUV induced photochemistry at solid surfaces. Time-of-flight mass spectroscopy (TOFMS) using the single-bunch operation of a synchrotron radiation source is a highly sensitive and convenient method for investigating the origin of PSD ions. This technique is particularly suitable for the boron-based system with a low photoabsorption cross section. The other advantage of this experimental approach is that the TOF spectrum can be used to evaluate PSD from solid surfaces and photolysis of gas molecules simultaneously, and its usage has recently been extended to the identification of intermediates formed during SR–CVD.[9,10] The signals due to surface-originating ions can be easily distinguished from those due to gas-originating ions because the former signals are discrete sharp peaks, whereas the latter signals form a broad band with poor mass resolution. In the present study we performed TOFMS measurement to investigate the photochemistry of $B_{10}H_{14}$ at semiconductor surfaces. Though we could not detect neutral products, the intermediate species resulting from PSD and from photolysis have been unambiguously identified, and we use these results here to speculate possible pathways of B film growth.

II. EXPERIMENT

Experiments were performed on the beam line 1C at the Photon Factory in the National Laboratory for High Energy Physics. SR emitted from the bending magnet is reflected, with a grazing incident angle of 4 deg, by a Pt-coated SiC mirror and directed onto the target surface. Figure 1 shows the energy distribution of the white SR beam along with the photoabsorption cross sections of Si and B atoms which were calculated from the data tables by Henke *et al.*[11] A carbon filter inserted in the beam line cut off most of the photons below 100 eV in order to cause reactions due to core electron excitation. The energy distribution of our SR beam thus started from 100 eV and the photon fraction decreased with increasing energy.

Details of the experimental procedure using the single-bunch mode of the positron storage ring (at a repetition cycle of 624 ns and with a ring current between 30 and 50 mA) are described elsewhere.[9,10] The TOFMS detector and the measuring system are shown schematically in Fig. 2. SR is irra-

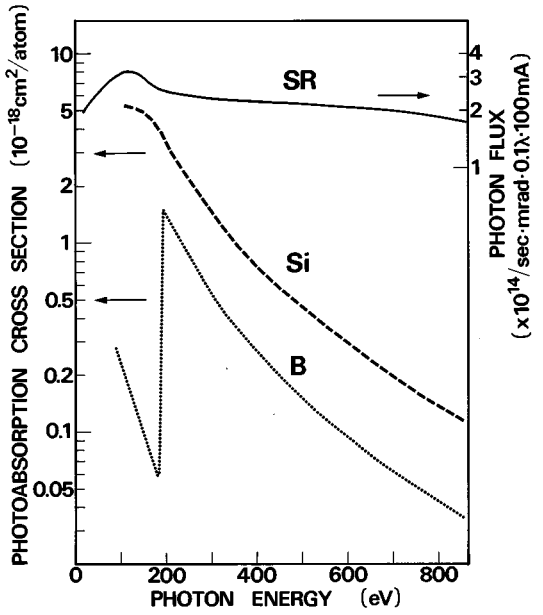

FIG. 1. Energy distribution of the SR beam along with photoabsorption cross section of B and Si atoms.

diated from the glancing direction to the surface plane, and the incident angle measured from the surface normal is designated θ_i. The PSD ions from the surface and fragment ions created by photolysis of $B_{10}H_{14}$ gas are collected into the drift tube through the grid mesh and are detected by the fast-response microchannel plate (MCP). The bias voltage applied to the substrate was +4.5 kV and the voltage applied to the grid mesh and the drift tube was −1.5 kV. The time

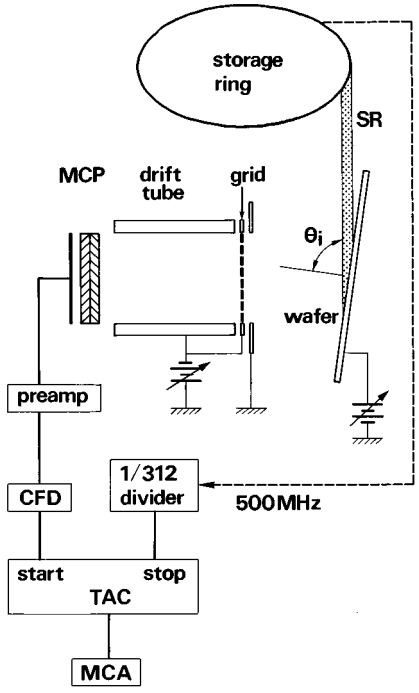

FIG. 2. Schematic drawing of the TOFMS detector and the block diagram of the measurement system.

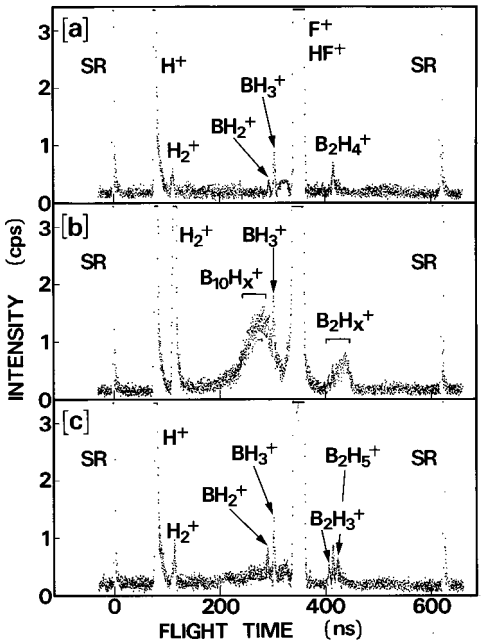

FIG. 3. Typical spectra obtained at $\theta_i=80°$ (a) from $B_{10}H_{14}$ adsorbed Si(100), (b) during SR–CVD in ambient $B_{10}H_{14}$ (9×10^{-6} Torr), and (c) from an B:H film grown by SR–CVD.

difference between the trigger signal (obtained by dividing the 500 MHz standard reference by 1/312) and the ion signal converted to a logic signal through a constant fraction discriminator (CFD) is measured by a biased time-to-amplitude converter (TAC). The spectra are stored in a multichannel analyzer (MCA). The resolution of the detector was 270 ps.[10]

Two in., *p*-type (1–10 Ω cm) Si(100) wafers were used as substrates. Native oxide formed when the wafers were rinsed in a $NH_4OH:H_2O_2:H_2O$ solution was evaporated by annealing them at 1000 °C under ultrahigh vacuum (UHV). The surface was shown by Auger electron spectroscopy (AES) to be atomically clean and by reflection high-energy electron diffraction (RHEED) to be well ordered. Crystalline $B_{10}H_{14}$ is stable at room temperature and decomposes at temperatures above 170 °C.[12] The $B_{10}H_{14}$ gas in these experiments was obtained by heating a stainless steel bottle of solid $B_{10}H_{14}$ at 70 °C.

III. RESULTS

Figure 3(a) depicts a typical TOFMS spectrum of PSD ions from $B_{10}H_{14}$-adsorbed Si(100). The $B_{10}H_{14}$ exposure was 2×10^3 langmuirs (1 L$=10^{-6}$ Torr s) and the background pressure during the TOF measurement was 4×10^{-9} Torr. The ion species appear between the two SR photon signals. The most intense signal was that of H^+ and the next most intense were those of F^+ and HF^+. The H^+ signal was 500 times more intense than the H_2^+ signals, but this is not evident in Fig. 3(a) because the vertical axis is expanded to show the low-intensity signals. It is known that the ion desorption probabilities of F atoms and H atoms bound to the F atoms are very high.[13] These ions can be observed even when an as-cleaned Si(100) surface is examined,[9] so the

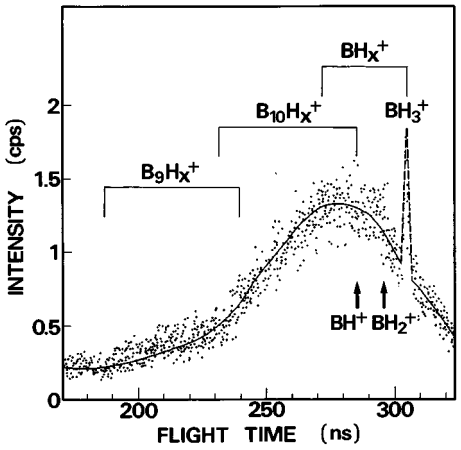

FIG. 4. The expanded spectrum for the region of interest including gas-phase product ions. The dashed curve shows the BH_3^+ PSD ion peak and the solid curve is the envelope of the product ions produced from gas-phase photolysis.

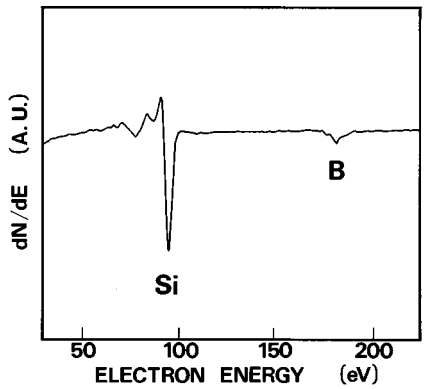

FIG. 5. Auger electron spectrum obtained after deposition of a thin B film on Si(100).

bonding partner of the desorbed H atoms must be assigned carefully. Considering the low photoabsorption coefficient of B (evident from Fig. 1), we expect the probability of H^+ being produced from $B_{10}H_{14}$ by direct photoexcitation to be very low. The substrate-mediated secondary process, however, could efficiently induce H^+ ejection. At least we can say that, in the present system, the possible bonding partners are Si, B, and F atoms.

The H_2^+, $^{11}BH_3^+$, and $^{11}B_2H_4^+$ signals are also clearly identifiable, and the $m/e=13$ signal is discernible. Just as reported in Perkins *et al.*,[7] the boron AES signal could not be observed from the sample surface. But detecting PSD signals specific to $B_{10}H_{14}$ confirms that a small amount (less than 0.1 monolayer) of $B_{10}H_{14}$ molecules does exist at the surface. Since the natural ratio of ^{11}B and ^{10}B is 4:1, the $m/e=13$ signal is contributed by $^{10}BH_3^+$ whose intensity is just a quarter of the $m/e=14$ signal (due mostly to $^{11}BH_3^+$). The $m/e=13$ signal intensity is actually much higher than that predicted from the isotope distribution, confirming that $^{11}BH_2^+$ is included in the $m/e=13$ signal.

Figure 3(b) shows a TOF spectrum measured during SR–CVD with a $B_{10}H_{14}$ pressure of 9×10^{-6} Torr. Under this $B_{10}H_{14}$ gas pressure the growing surface will be passivated by $B_{10}H_{14}$ adlayers. It is seen that a broad band of ion signals resulting from photolysis of $B_{10}H_{14}$ is superimposed on the discrete signals of PSD ions. Because ionization of gas molecules can occur everywhere within the SR beam path, the flight length of each of the ionized molecules has a finite distribution, and consequently the mass resolution is degraded. This apparently disadvantageous characteristic is useful in distinguishing PSD ions from those created in the gas phase. Figure 4 shows the expanded TOF spectrum for the time region where signals of gas-phase product appear. The contribution of the surface-originating BH_3^+, for instance, can be isolated by subtracting the envelope curve of the bunch signals of gas origin. The mass positions for $^{11}BH_2^+$ and $^{11}BH^+$ are indicated by arrows and these PSD ion signals are unclear.

Another problem in signal assignment is that the signals of species with flight times of t ns and $(t+624)$ ns appear at the same position due to the wrap around effect. The BH_x^+ $(x=0–3)$ signals should appear between 271 and 305 ns, and $B_{10}H_x^+$ $(x=0–14)$ signals should appear between 231 and 284 ns. The two regions overlap from 271 to 284 ns. Although the mass resolution is not satisfactory, the predominant part of the signal bunch between 230 and 271 ns is due to $B_{10}H_x^+$ and that of the part between 284 and 315 ns is due to BH_x^+. $B_2H_x^+$ $(x=0–6)$ signals should appear between 382 and 431 ns. The slightly increased intensity near 430 ns in Fig. 3(b) as compared with Fig. 3(a) indicates detection of $B_2H_5^+$ and $B_2H_6^+$ ions. $B_9H_x^+$ $(x=0–13)$ signals should appear between 187 and 239 ns, and $B_8H_y^+$ signals should appear between 141 and 192 ns. The $B_9H_x^+$ signals are obviously present at the shoulder of the bunch of $B_{10}H_x^+$, but the S/N ratio is too low for $B_8H_x^+$ to be detected. The poor mass resolution of $B_{10}H_x^+$ and $B_9H_x^+$ is also due to the very small flight time difference for ions of similar masses.

Figure 5 shows an AES spectrum from the irradiated region on the Si wafer after 2 h of SR–CVD. In addition to the elementary Si signal at an electron energy of 92 eV, the B signal at 179 eV is evident. The B signal for the nonirradiated region was below the detection limit even though a submonolayer thickness of $B_{10}H_{14}$ should have been adsorbed there. This B signal, detectable only in the irradiated region, indicates the presence of a boron film grown by SR–CVD. Because the film was grown at room temperature, H atoms may be incorporated into it as they are into Si films grown by SR–CVD.[5] The average thickness of the B film estimated from the B and Si Auger signal intensities is 2.8 Å, which corresponds to two monolayers or less.

The TOF spectrum of PSD ions from the B:H surface is shown in Fig. 3(c), where it is clear that the broad band of signals is absent in the absence of $B_{10}H_{14}$ gas. The qualitative difference from PSD at the $B_{10}H_{14}$-adsorbed Si(100) [Fig. 3(a)] is that signals from $B_2H_3^+$ and $B_2H_5^+$ species appear. The increased variation in the cracking pattern indicates that the B:H surface consists of a complicated network that decomposes into various cracking fragments. Repeating

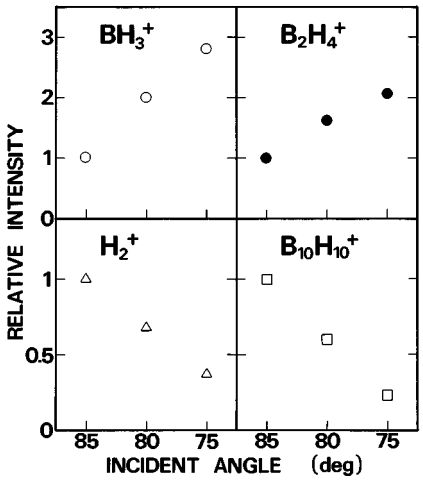

FIG. 6. Ion intensity vs. SR incident angle (measured from the surface normal).

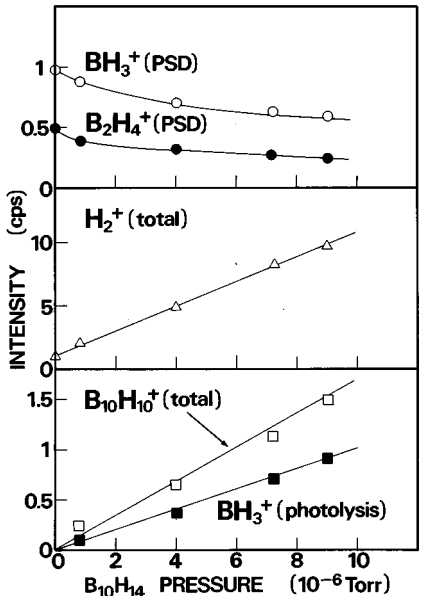

FIG. 7. Ion intensity vs. $B_{10}H_{14}$ pressure during SR–CVD. Lines are guide to the eye.

reactive sticking of B hydride radicals (ions) on the B:H surface will produce ramified B chains.

To acquire further information on the desorption kinetics, we evaluated the relation between θ_i and the intensities of the PSD ions from the B:H surface. The intensities of H_2^+, BH_3^+, and $B_2H_4^+$ signals were measured in UHV, and the $B_{10}H_{10}^+$ intensity at the flight time of 270 ns was measured under low $B_{10}H_{14}$ pressure (1×10^{-6} Torr) so that the contribution from the $B_{10}H_{14}$ adlayers became predominant. The results are shown in Fig. 6 after normalization with the intensity measured at $\theta_i=85°$. Almost all emitted ions were collected because of the high electric field applied between the substrate and the grid mesh, so the detection efficiency was insensitive to changes in θ_i between 75° and 85°.

The intensities of BH_3^+ and $B_2H_4^+$ ions increased with increasing θ_i, whereas those of H_2^+ and $B_{10}H_{10}^+$ decreased. The rather abrupt intensity change confirms that it is not caused by the detection efficiency change. Following the general rule when VUV and soft x-ray are incident on solid surfaces, the photoreflectivity increases with increasing θ_i. That is, the number of photons penetrating the bulk decreases. For photons with a given wavelength, the proportion of surface excitation becomes maximum at a critical incident angle of total reflection. The θ_i dependence of the H_2^+ and $B_{10}H_{10}^+$ intensities is consistent with the surface excitation mechanism and is evidence that most of the H_2^+ and $B_{10}H_x^+$ are produced by dissociative photoionization followed by direct photoabsorption of $B_{10}H_{14}$ adlayer molecules. Oppositely, the θ_i dependence of the BH_3^+ and $B_2H_4^+$ intensities implies that the ionization producing these species is predominantly due to substrate excitation. The possible excitation sources are photoelectrons, Auger electrons, and secondary electrons backscattered from the bulk.

The intensities of the ion signals during SR–CVD are plotted in Fig. 7 as a function of $B_{10}H_{14}$ pressure. The $B_{10}H_{10}^+$ intensity is exactly proportional to pressure, indicating that $B_{10}H_{10}^+$ is generated from $B_{10}H_{14}$. When the gas pressure is low, the number of $B_{10}H_{14}$ molecules trapped at the surface is proportional to pressure. Thus the two origins (gas and adsorbate) are not distinguished from the pressure dependence alone. Similarly, the H_2^+ intensity depends linearly on pressure. The nonzero offset at zero pressure is due to stimulated ejection of H_2^+ from molecularly adsorbed $B_{10}H_{14}$ that does not disappear upon evacuation. The proportionality to pressure, on the other hand, corresponds to the dissociative photoionization of $B_{10}H_{14}$ gas molecules, releasing H_2^+. In contrast, the intensities of the BH_3^+ and $B_2H_4^+$ PSD ions decreased with increasing pressure, while the BH_3^+ intensity of the gas origin was proportional to pressure.

Figure 8 shows H^+ and H_2^+ signals extracted from the spectra shown in Figs. 3(b) and 3(c). The bimodal shape of the H^+ peak indicates presence of two distinct chemical states, and the different flight times result from different Coulomb repulsion energies when the ions are ejected. The two chemical states of H^+ PSD ions from SiH_x-adsorbed Si (100) have been tentatively assigned to Si–H and F–H.[9,10] Apparently, the peak intensity of H^+ under UHV was nearly the same as it was during SR–CVD, whereas the H_2^+ intensity increased enormously. The intact H^+ yield implies that H^+ desorption from B–H bond contributes negligibly, consistent with the low photoabsorption of B atoms. Most part of H^+ comes from either Si–H or F–H bonds. Another possible interpretation is that some of the H^+ ions emitted from the B film surface were neutralized by collision with $B_{10}H_{14}$ molecules and their intensity decreased, but this attenuation was compensated by the increased H^+ ions created by photolysis. It is worth noting that the H^+ and H_2^+ signals measured during SR–CVD have enhanced tails toward longer flight times (indicated by arrows). This portion of signal, though small, is obviously contributed by the gas-phase product ions generated at the remote part from the sample surface. These enhanced tails confirm that H^+ is produced from $B_{10}H_{14}$.

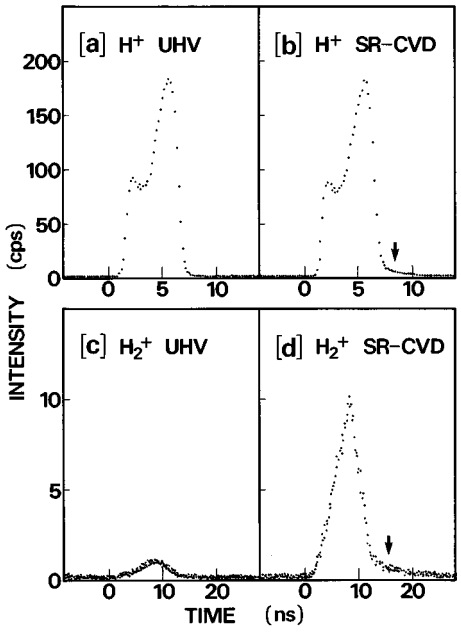

FIG. 8. The high-resolution spectra of H^+ and H_2^+ ions during SR–CVD and after evacuation. The spectra during SR–CVD have tails indicated by arrows.

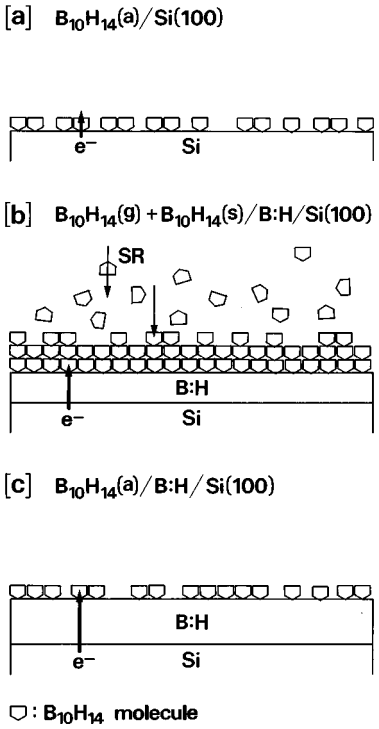

FIG. 10. Schematic representation of the surfaces corresponding to the spectra shown in Fig. 3.

IV. DISCUSSION

A. $B_{10}H_{14}$-surface interaction and photoabsorption by $B_{10}H_{14}$

Before discussing the photochemistry of $B_{10}H_{14}$ on Si(100), chemisorption and photoabsorption of $B_{10}H_{14}$ should be surveyed. Lee *et al.*[14] calculated the optimum geometry for $B_{10}H_{14}$ by using a modified neglect of differential overlap (MNDO) calculation, and the resultant structure is illustrated in Fig. 9. The cluster molecule has a cage structure with ten B–H single bonds and four B–H–B bridge bonds. Hereafter, we designate $B_{10}H_{14}$ molecules in the ambient, chemisorbed on the surface, and physisorbed on the surface respectively as $B_{10}H_{14}(g)$, $B_{10}H_{14}(a)$, and $B_{10}H_{14}(s)$. It is known that closed boran cage molecules are less reactive than framework boron hydrides. Previous studies of $B_{10}H_{14}(a)$/Si(111) using electron energy loss spectroscopy (EEELS)[14] and ultraviolet photoelectron spectroscopy (UPS),[15] revealed that at room temperature $B_{10}H_{14}$ adsorbs molecularly. Avouris *et al.*[16] observed a clear round disk image of $B_{10}H_{14}(a)$ on Si(111) by scanning tunneling microscopy (STM), and they found that $B_{10}H_{14}$ molecules adsorb preferentially on defects and on center adatoms of the Si(111)-7×7 surface. Weak adsorption due to the van der Waals force is facilitated by the larger molecular weight (112.2) of $B_{10}H_{14}$. Following the random sticking of the large size molecule, considerable numbers of Si dangling bonds remain unsaturated. Also on the Si(100)-2×1 surface we confirmed that the amount of $B_{10}H_{14}$ was below the detection limit by AES. This situation is illustrated in Fig. 10(a). The configuration of the adsorption state has not yet been determined. Although we cannot rule out the possibility that part of $B_{10}H_{14}(a)$ is dissociated, the spectrum in Fig. 3(a) primarily represents the desorption products from $B_{10}H_{14}(a)$.

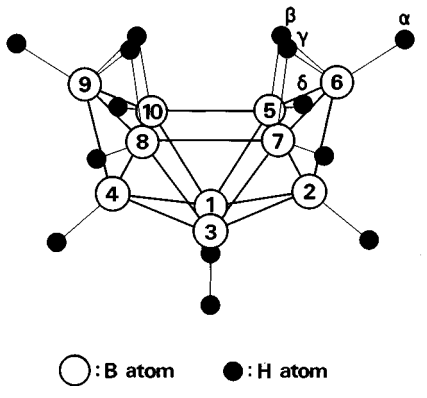

FIG. 9. Schematic description of a $B_{10}H_{14}$ molecule.

As seen from Fig. 1, excitation of Si($2p$) and B($1s$) core electrons occurs at photon energies higher than 100 and 195 eV, respectively. The effective photoabsorption by Si atom starts from 100 eV because the photons below 100 eV were cut off. The cross section is especially high between 100 and 200 eV. Within this energy range the cross section for B is 30–100 times lower than that for Si, and therefore most of the low-energy photons are absorbed by substrate Si atoms. Electronic excitation of the adsorbate is largely an indirect process induced by photoelectrons, Auger electrons, and secondary electrons backscattered from the Si substrate. This is especially true for $B_{10}H_{14}(a)$/Si(100) because the Si substrate is a semi-infinite medium whereas $B_{10}H_{14}(a)$ does

not even form a continuous layer. The findings by Rosenberg *et al.*[6,7] that the B film grows exclusively in the irradiated region is supported by this reasoning.

B. Photon-stimulated desorption

The desorption species characteristic of $B_{10}H_{14}(a)$/Si(100) have been found to be H_2^+, BH_2^+, BH_3^+, and $B_2H_4^+$. These are ionic from birth and are not desorbed neutrals that are subsequently photoionized by the same SR pulse. This can be easily seen from Fig. 7. The intensity of BH_3^+ PSD ions is 1 cps under the UHV (4×10^{-9} Torr) condition. SR irradiation caused absolutely no increase in the pressure. On the other hand, to gain the same BH_3^+ yield from photolysis, the ambient $B_{10}H_{14}$ pressure of 1×10^{-5} Torr is required. Hence the contribution of the latter post-ionization channel is less than 0.04%, if present. This does not mean, however, that ionic fragments are representative of the overall desorption. Because the chemical bond involved in the present system are covalent, neutral desorption will be dominant. The branching ratio for the PSD species may differ between ions and neutrals, but the following discussion characterizes the ionic desorption process specific to $B_{10}H_{14}$/Si(100).

According to the general principle for PSD, the probability of positive ion production increases with increasing ionicity of the chemical bond. The Knotek–Feibelman mechanism[17] applies to largely electronegative fluorine atoms: H^+ desorption from F–H bond occurs highly efficiently following the reversal of the Madelung potential associated with Auger decay of the core hole.[13] The Pauling electronegativities of B, Si, and H atoms are respectively 2.0, 1.8, and 2.1. The difference between the electronegativities of B and H is only 0.1, which means that the B–H bond is extremely covalent. Similarly, the electronegativity differences for Si–H and Si–B bonds are respectively only 0.3 and 0.2, and these bonds are also covalent. For ion desorption from covalent materials to occur, multiple holes must be localized long enough in the valence orbital countering the fast hopping decay of the holes. Creating double or multiple holes is required in some systems.[18,19] The extreme covalency of the B–H bond and the low photoabsorption by B atoms account for the fundamentally low desorption probability of H^+ bound to B atoms. Furthermore, electrons in the B–H–B bridge bonds and B–B bonds that hold the cage structure together are nonlocalized within the molecule, and this feature is also disadvantageous for bond rupture driven by valence holes localized in a single bond. H atoms already present on Si(100) after the surface cleaning procedure and those dissociated from $B_{10}H_{14}$ form the Si–H bonds, which are slightly more ionic than B–H bonds and make sizeable contribution to the H^+ signal.

The H_2^+ desorption is explained in a way similar to that used to explain the desorption of H_2^+ from Si_2H_6-chemisorbed Si(100), where H_2^+ desorbs preferentially from Si dihydrides [$SiH_2(a)$].[9] Even if $B_{10}H_{14}(a)$ is partially dissociated on Si(100), the released H atoms are not likely to form $SiH_2(a)$. Then H_2^+ will originate from $B_{10}H_{14}(a)$. Consider the B(6) atom site indicated in Fig. 9, where one H(α) atom terminates the B(6) atom and two H(β) and H(τ) atoms bridge to the other B atoms. This H–B–$(H-)_2$ site can be regarded an admolecule to the parent $B_{10}H_{14}$. If the character of an electronically excited state localized at the H–B–$(H-)_2$ site is antibonding for the B–H bonds and bonding between the two H atoms, the excited admolecule can be dissociated by releasing H_2^+. This reaction can be induced by direct photoexcitation and is consistent with the result in Fig. 6.

With regard to SiH_x-adsorbed Si(100), the only desorption species are H^+ and H_2^+, and Si-containing ions such as SiH_2^+ and SiH^+ are never observed.[9,10] For ejection of SiH_x^+, two covalent Si–Si back bonds between an admolecule and the substrate must be broken. The probability of this is extremely low because of the efficient hopping decay of the valence holes promoted by nonlocalized electrons in the substrate. The situation is entirely different for the $B_{10}H_{14}$ molecularly adsorbed on Si(100), since the $B_{10}H_{14}$ molecule–surface interaction is weak. The ion survival probability of PSD ions will be high when it desorbs from a B–H bond far from the surface. The B–H bond is less affected by the presence of the substrate because the interaction strength between the ligand and the surface decays exponentially according to the distance between them.

Different from $SiH_x(a)$/Si(100), boron containing ions (BH_2^+, BH_3^+, and $B_2H_4^+$) have been detected from $B_{10}H_{14}(a)$/Si(100) with intensities comparable to that of H_2^+. That the intensities of these signals are far lower than that of H^+ is consistent with the low photoabsorption cross section of B atoms. These species may originate from the BH_x ligand extending into the vacuum. The appearance of only limited kinds of cracking products implies selective breaking of chemical bonds, and this can be explained by examining Fig. 9. If the B(6) atom desorbs accompanied by all three H(α), H(β), and H(τ) atoms bound to it, BH_3^+ is created. If the B(5) and B(6) atom pair desorbs accompanied by all four H(α), H(β), H(τ), and H(δ) atoms bound to the B atoms, $B_2H_4^+$ is created. For this to occur, three B–B bonds must be broken to create BH_3^+, and four B–B bonds must be broken to create $B_2H_4^+$. Auger decay of core holes associated with shake-up or shake-off resonance[18,19] can generate localized multiple holes within a $B_{10}H_{14}$ parent molecule. The θ_i dependence of the desorption yields of BH_3^+ and $B_2H_4^+$, however, suggests substrate-mediated desorption kinetics. Electron impact ionization will significantly promote multiple hole creation. The excited molecules are decomposed into small fragments by the ''Coulomb explosion'' mechanism.

The attenuation of the BH_3^+ and $B_2H_4^+$ PSD ion yields with increasing $B_{10}H_{14}$ pressure (Fig. 7) can be explained in two ways. First, secondary electrons emitted from the Si substrate are attenuated by the $B_{10}H_{14}$ adlayers, which reduces the probability of electron-stimulated positive ion formation from the $B_{10}H_{14}$ molecules at the outermost surface. Second, the PSD ions produced at the a–B:H surface or inside the film are partially neutralized when passing through the $B_{10}H_{14}$ adlayers before being ejected into the vacuum. This kind of attenuation was first reported by Sack *et al.*,[20] who studied electron-stimulated O^+ desorption from a O/W(100) surface covered with rare gas films. They observed that the

O^+ yield decreased exponentially with increasing thickness of the condensed rare gas layer.

During SR–CVD the Si(100) surface is eventually covered by a B:H film. After the gas is evacuated, less than a monolayer of $B_{10}H_{14}(a)$ will remain on the B:H surface as illustrated in Fig. 10(c). As seen from Fig. 3(c), PSD from the B:H film is associated with $B_2H_3^+$ and $B_2H_5^+$ and all ion intensities are greater than those observed from $B_{10}H_{14}(a)$/Si(100). The additional species may be responsible for decomposition of higher-order boron hydrides covering the B:H film. If the B:H film has a ramified B network due to fractal growth, bond breaking at several sites will generate a variety of B hydride species.

C. Deposition pathway of boron films

The low vapor pressure of $B_{10}H_{14}$ implies that the surface of the deposited B:H film will be covered with $B_{10}H_{14}$ multiple adlayers $[B_{10}H_{14}(s)]$ during SR–CVD, and this situation is illustrated in Fig. 10(b). $B_{10}H_{14}(g)$ and $B_{10}H_{14}(s)$ are in adsorption–desorption equilibrium and the photolysis of both species must be considered. The primary decomposition products are H_2^+, $B_{10}H_x^+$, BH_x^+, and $B_9H_x^+$. The primary photolysis during SR–CVD is expressed (neglecting the charge state of the products)

$$B_{10}H_{14}(g)(s)+h\nu \rightarrow B_{10}H_x+\mathrm{mH(or\ H_2)} \rightarrow BH_x+B_9H_y. \quad (1)$$

Only stripping H atom(s) by breaking single B–H bonds can produce $B_{10}H_x$. The simple Auger stimulated decomposition mechanism by exciting a $B(1s)$ core electron can account for the formation of $B_{10}H_x^+$. Formation of BH_x^+ and $B_9H_x^+$ ions, however, requires simultaneous breaking at least three B–B bonds, and Coulomb explosion mechanism involving multiple excitation is inferred.

Since BH_x^+, $B_9H_x^+$, and $B_{10}H_x^+$ have been detected at reasonable intensities, one might conclude that they are the precursors for deposition. These species produced from $B_{10}H_{14}(g)$, however, must pass through the $B_{10}H_{14}$ adlayers before sticking to the B:H surface, and may be repelled in a half way. If they are produced from $B_{10}H_{14}(s)$, they can interact with the surface instantaneously. The problem here is that mutual rebonding of the large radicals (B_9H_x and $B_{10}H_x$) and subsequent transformation to B network will be difficult because the cage structure of a $B_{10}H_{14}$ molecule does not directly correlate to the B film network. Even if these radicals stick to a substrate B atom, the large admolecule connected to the surface through a single bond will be unstable and again be liberated by electronic excitation. In this respect, BH_x is the likeliest candidate for the precursors, but we cannot exclude B_9H_x and $B_{10}H_x$ as possible intermediates in the growth of the B film. If the products generated from $B_{10}H_{14}(g)$ are precursors, B film deposition should occur in the nonirradiated region to some extent and this is inconsistent with the observations reported in Refs. 6 and 7. Confirmation of region-selectivity, however, would require measurement of a thickness profile, extending across irradiated and nonirradiated regions, after deposition of a thick B film. Strictly speaking, any judgement on the selectivity is uncertain until aspect ratio between the two regions is evaluated quantitatively.

An alternative source for the precursors to the B growth is $B_{10}H_{14}(s)$ decomposition, stimulated by backscattered electrons, to small fragments such as BH_x and B_2H_x. The BH_2^+, BH_3^+, and $B_2H_4^+$ PSD ions detected in the present work could be such fragments failed to be incorporated. The small fragments could readily bind one another and be incorporated in the B network, and the hydrogenated film will further release H and H_2, either thermally or stimulated by SR, and be transformed to B films containing less hydrogen atoms.

V. SUMMARY

The species involved in PSD and photolysis from $B_{10}H_{14}$ at solid surfaces have been clarified by means of single-bunch TOFMS. The PSD species characteristic for $B_{10}H_{14}(a)$/Si(100) are H_2^+, BH_2^+, BH_3^+, and $B_2H_4^+$, whereas the photolysis species from $B_{10}H_{14}(g)$ and $B_{10}H_{14}(s)$ during SR-excited B film deposition are H_2^+, $B_{10}H_x^+$, BH_x^+, and $B_9H_x^+$. These photolysis ion signals form a broad band superimposes on the sharp peaks of the PSD ions. From $B_{10}H_{14}(a)$/B:H/Si(100), PSD of $B_2H_3^+$ and $B_2H_5^+$ were additionally observed. The cracking patterns are correlated with the $B_{10}H_{14}$ structure. It is worth noting, however, that the observed branching ratio is specific to ions and could be significantly different for neutrals which were not detected in this study. The θ_i dependence of the ion yields indicates that H_2^+ and $B_{10}H_x^+$ are produced by direct photolysis and that BH_3^+ and $B_2H_4^+$ are produced by substrate-mediated secondary processes. During SR–CVD the intensities of BH_3^+ and $B_2H_4^+$ PSD ions decreased with increasing $B_{10}H_{14}$ pressure. The intensities of H_2^+ and $B_{10}H_x^+$, in contrast, increased linearly with pressure. The deposition of the B film probably proceeds either by means of reactive sticking of photolysis products such as BH_x, B_9H_x, and $B_{10}H_x$ or by means of secondary-electron-induced decomposition of $B_{10}H_{14}(s)$ into small fragments that subsequently rebond.

ACKNOWLEDGMENTS

We thank S. Ishihara and T. Hosokawa for supporting our studies. We also thank Professor Ken'ichiro Tanaka for his suggestion to use the single bunch mode.

[1] H. Akazawa, Y. Utsumi, T. Urisu, and M. Nagase, Phys. Rev. B **47**, 15946 (1993).
[2] H. Akazawa, M. Magase, and Y. Utsumi, Appl. Phys. Lett. **64**, 754 (1994).
[3] H. Akazawa, Y. Utsumi, and M. Nagase, Appl. Surf. Sci. **79/80**, 299 (1994).
[4] H. Akazawa, Appl. Surf. Sci. **82/83**, 394 (1994).
[5] H. Akazawa and Y. Utsumi, J. Appl. Phys. **78**, 2725 and 2740 (1995).
[6] R. A. Rosenberg, F. K. Perkins, D. C. Mancini, G. R. Harp, B. P. Tonner, S. Lee, and P. A. Dowben, Appl. Phys. Lett. **58**, 607 (1991).
[7] F. K. Perkins, R. A. Rosenberg, S. Lee, and P. A. Dowben, J. Appl. Phys. **69**, 4103 (1991).
[8] M. W. Ruckmam, M. F. Murray, J. K. Mowlem, and D. R. Strongin, J. Vac. Sci. Technol. A **11**, 2477 (1993).
[9] H. Akazawa, Phys. Rev. B **51**, 7314 (1995).

[10] H. Akazawa, Nucl. Instrum. Meth. B **101**, 227 (1995).
[11] B. L. Henke, P. Lee, T. J. Tanaka, R. L. Shimabukuro, and B. K. Fujikawa, At. Data Nucl. Data Tables **27**, 1 (1982).
[12] Y. G. Kim, P. A. Dowben, J. T. Spencer, and G. O. Ramseyer, J. Vac. Sci. Technol. A **7**, 2769 (1989).
[13] Ph. Avouris, F. Bozso, and A. R. Rossi, in *Photon Beam and Plasma Stimulated Chemical Processes at Surfaces*, edited by V. M. Donnelly, I. P. Herman, and M. Horose, MRS Symposia Proceedings, No. 75 (Material Research Society, Pittsburgh, 1987), p. 591.
[14] S. Lee, P. A. Dowben, A. T. Wen, A. P. Hitchcock, J. A. Glass, Jr., and J. T. Spencer, J. Vac. Sci. Technol. A **10**, 881 (1992).
[15] S. Lee, D. Li, S. M. Cndrowski-Guillaume, P. A. Dowben, F. K. Perkins, S. P. Frigo, and R. A. Rosenberg, J. Vac. Sci. Technol. A **10**, 2299 (1992).
[16] Ph. Avouris, I.-W. Lyo, F. Bozso, and E. Kaxiras, J. Vac. Sci. Technol. A **8**, 3405 (1990).
[17] M. L. Knotek and P. J. Feibelman, Surf. Sci. **90**, 78 (1979).
[18] L. Hellner, L. Philippe, G. Dujardin, M.-L. Ramage, M. Rose, P. Cirkel, and P. Dumas, Nucl. Instrum. Meth. B **78**, 342 (1993).
[19] H. Ikeura, T. Sekiguchi, K. Tanaka, K. Obi, N. Ueno, and K. Honma, Jpn. J. Appl. Phys. **32**, 246 (1993).
[20] N. J. Sack, M. A. Akbulut, and T. E. Madey, Phys. Rev. Lett. **73**, 794 (1994).